Journal of Aircraft
Vol. 31, No. 1, Jan.–Feb. 1994

Simulation Model for Tail Rotor Failure

Matthew J. O'Rourke*
Lockheed Engineering and Sciences Company, Hampton, Virginia 23665

Tail rotor failure in a helicopter can be a very dangerous and unstable condition. For this reason a helicopter simulation model, DYN, has been formulated to analyze helicopter flight response to tail rotor failure and steady flight recovery. This model uses classical rotor theory and integrates the nonlinear Euler equations of motion. DYN has been validated against flight tests in several flight regimes in response to all three main rotor controls. The helicopter used for the validation is the McDonnell Douglas AH-64A Apache. The validation also compares dynamic response to FLYRT, the McDonnell Douglas AH-64A flight simulation model. The results of the validation show fairly good agreement with flight test, and even better agreement with FLYRT. Analysis of aircraft response following a tail rotor failure shows the potentially catastrophic nature of this kind of failure. With the use of some basic feedback control, however, the helicopter may be recovered with some descent rate and forward airspeed. The relationship between forward airspeed and descent rate needed for trimmed flight without a tail rotor is established at the conclusion of this study.

Nomenclature

a_1 = longitudinal rotor flapping
b_1 = lateral rotor flapping
D = main rotor diameter
F_X = force acting along X-body axis
F_Y = force acting along Y-body axis
F_Z = force acting along Z-body axis
G_P = roll rate feedback gain
G_Q = pitch rate feedback gain
G_V = velocity feedback gain
G_{yd} = heading feedback gain
G_β = sideslip feedback gain
G_Θ = pitch angle feedback gain
G_Φ = roll angle feedback gain
I_X = X-body axis moment of inertia
I_{XZ} = roll-yaw inertial coupling
I_Y = Y-body axis moment of inertia
I_Z = Z-body axis moment of inertia
L = rolling moment
M = pitching moment
m = mass
N = yawing moment
P = roll rate
Q = pitch rate
R = yaw rate
T_{MR} = main rotor thrust
u_f = velocity along X-body axis
V = velocity
V_D = vertical descent rate
v_f = velocity along Y-body axis
w = main rotor downwash velocity
w_f = velocity along Z-body axis
X = X-body coordinate
x = X-global coordinate
Y = Y-body coordinate
y = Y-global coordinate
$\dot{y}$ = translation rate along Y-global axis
Z = Z-body coordinate
z = Z-global coordinate
α = angle of attack
β = sideslip angle, main rotor flapping angle
β_0 = main rotor coning angle
Γ_0 = rotor trailing vortex strength
ΔV = velocity error
$\Delta\beta$ = sideslip error
$\Delta\Theta$ = pitch angle error
$\Delta\Phi$ = roll angle error
Θ = pitch Euler angle
θ = local rotor pitch
θ_0 = collective pitch
θ_1 = lateral cyclic pitch
θ_2 = longitudinal cyclic pitch
Φ = roll Euler angle
ρ = air density
Ψ = yaw Euler angle
ψ = rotor azimuth angle

Superscripts

$\dot{}$ = first derivative with respect to time
$'$ = wind axes coordinates

Introduction

THE helicopter, with its tail rotor fully operational, typically is unstable without substantial forward speed. Therefore, it is clear that a full or even partial tail rotor failure can cause significant control problems at best. A study from 1980 to 1985[1] indicates that for scout and attack helicopters, 32% of all accidents due to subsystem malfunctions (i.e., excluding pilot error) are caused by tail rotor failures. The helicopter used in this study, the McDonnell Douglas AH-64A Apache, has experienced only four fatal crashes in its career to date. Two of these accidents were due to tail rotor failure (swash plate seizure and tail rotor separation).

Knowing the seriousness of tail rotor failure, it is desired to outline why tail rotor failure is a problem and how the controllability of the helicopter can be assessed. When the tail rotor fails, the airframe of most American helicopters will respond to the excess positive torque generated by the main rotor by yawing nose right (negative sideslip). Helicopters with vertical tails produce a negative torque, or antitorque, in negative sideslip which helps offset the main rotor torque. In most cases the amount of antitorque produced by the airframe is not sufficient to trim the helicopter in steady-level flight. If this is the case, the courses of action to achieve directional trim are limited. A reduction of main rotor col-

Received July 12, 1991; presented as Paper 92-4633 at the AIAA Atmospheric Flight Mechanics Conference, Hilton Head, SC, Aug. 10–12, 1992; revision received Sept. 4, 1992; accepted for publication Oct. 26, 1992.

*Senior Engineer Associate, Aeronautics Department. Member AIAA.

lective pitch will result in a reduction in main rotor torque. Additionally, the vertical stabilizer can be loaded by increasing negative sideslip and/or increasing airspeed. However, increasing sideslip and airspeed will further increase drag, resulting in increased main rotor power, and thus torque, to maintain a given directional trim condition. Keep in mind that all of this torque management is to be accomplished using controls that are much less effective directional controls than a tail rotor.

Previous studies[2,3] using static analyses have concluded that steady, level flight without a tail rotor is not possible at speeds near minimum power (70–80 kt) due to sideward flight requirements. In fact, the AH-64A was originally required to fly steady and level without a tail rotor at 80 kt. Reference 2 describes that the sideward flight requirement and the requirement for flight with no tail rotor could not be met simultaneously. Tail rotor blockage in sideward flight is the main reason for this due to the large vertical stabilizer needed to overcome the main rotor torque at 80 kt. In any case, conclusions were made in Ref. 2 that the AH-64A could maintain steady flight without a tail rotor at 80 kt with some descent, and at 125 kt steady and level.

When an actual tail rotor failure occurs, a statically trimmed solution may or may not be achievable due to the violent motion the helicopter may experience. This motion is due to the extreme yawing moment imbalance from the main rotor torque and rolling moment imbalance from main rotor lateral flapping. Thus, a dynamic model is needed to adequately assess the controllability of the helicopter and will allow analysis of the aircraft as it responds to the torque imbalance. The model also allows varying control inputs with time to drive the motion of the helicopter, determining if the steady-state solutions found in Ref. 2 are possible.

This article will discuss a helicopter simulation model developed to analyze tail rotor failure called DYN. It will present validation of the dynamic response of this model against flight tests for the AH-64A to ensure accuracy. It will then present several posttail rotor failure time histories without control to illustrate the severity of such failures. A closed-loop stability augmentation system will be developed to attempt recovery of the helicopter following the failure. The stability augmentation loop may be closed by an automatic control system, or as in this article, with a "paper pilot" which represents ideal pilot response. The main difference between the paper pilot and an automatic control system (in this investigation) is the lag time and immediate reaction between initial control inputs and the failure.

The purpose of this study is not to present one correct course of action following a tail rotor failure, nor is it to develop a control system to be implemented on an actual helicopter. Its purpose is, however, to provide a tool which can be used to test different control logic to more clearly define helicopter vulnerability without a tail rotor. Some general conclusions regarding tail rotor failure will be presented.

Helicopter Simulation Model

The helicopter simulation model is intended for use as a tool to assess the vulnerability of different existing helicopters in different mission scenarios. It was designed for ease of use, limiting the number of inputs and computational requirements. Every recourse to increase the noncomputation-intensive accuracy is taken. This calls for the use of classical rotor theory, modified where necessary, and utilization of available wind-tunnel and flight test information. The notation of Ref. 4 is adopted throughout this study. Care is taken not to dedicate the model to any particular helicopter. This requires that any influences such as detailed rotor wake influence on the empennage or unusual secondary control systems not be included.

Classical Rotor Theory

Classical rotor theory is discussed in detail in Ref. 4. In classical theory, the rotor is assumed fully rigid and is allowed to flap about the chordwise blade axis, and to pitch about the spanwise blade axis, without any lead-lag motion in the plane of rotation. It uses the flapping equation of motion of the blade with the control inputs and the aerodynamic conditions of the rotor disc defined by inflow ratio (the ratio flow velocity normal to the rotor disc to rotor tip speed) and rotor downwash velocity. This information is used to integrate the lift and drag along the blade and around the azimuth. It also uses basic momentum theory to predict rotor ideal power. The classical equations will not be derived since such a derivation is well-documented.[4] First harmonic rotor flapping (β) is assumed, and the governing equation describing it at any azimuthal station ψ (Fig. 1), is given as Eq. (1). The coning angle (β_0) is a constant for any steady rotor condition. This article assumes a quasisteady rotor, i.e., the rotor responds to control inputs much faster than the airframe. The basic equation describing main rotor pitch control θ, as a function of ψ is given in Eq. (2):

$$\beta = \beta_0 - a_1 \cos\psi - b_1 \sin\psi \tag{1}$$

$$\theta = \theta_0 + \theta_1 \cos\psi + \theta_2 \sin\psi \tag{2}$$

There are two main sources of rotor power required when considering classical theory. They are induced (ideal) power and blade profile power. From momentum theory, ideal power is the product of thrust and the net velocity normal to and down through the rotor tip path plane (swept out by the tips of the flapping rotor). Empirical evidence presented in Ref. 4 has shown that this relationship is between 10–15% too low, so the ideal value is increased by 12%. The profile power is calculated using the method outlined in Ref. 8. Some attempt was made to correct for compressibility and stall effects on rotor power required. These methods will not be discussed at this time, however, a full discussion is given in Ref. 4 and in the original work (Ref. 5).

Helicopter Airframe Forces and Moments

The helicopter airframe model accounts for the fuselage, a stub wing, a horizontal stabilizer/stabilator, and a vertical tail. Three-dimensional wind-tunnel data for the lift and drag of each lifting surface is input from -180 to $+180$ deg α. These angles of attack account for pitch and yaw rates at the empennage and allow the rate damping effects of the empennage to be accounted for. However, the fuselage model is somewhat more complex.

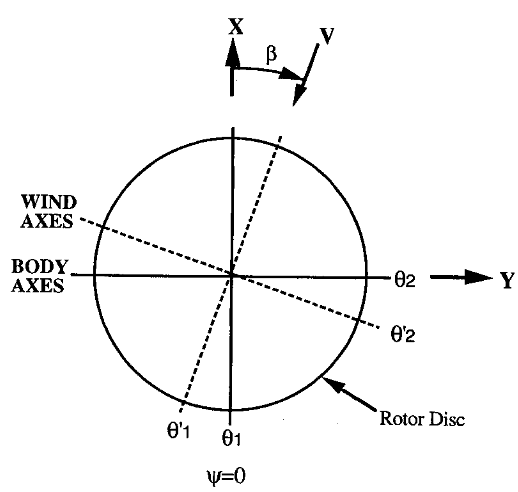

Fig. 1 Transformation of the cyclic main rotor controls to the wind axes.

The model for the helicopter fuselage was taken from the helicopter dynamic simulation model C-81.[6] This is also essentially the fuselage model used in FLYRT,[7] the McDonnell Douglas AH-64A simulation model. This fuselage model presented in this article consists of two parts. The first is a low α model which is simply a table lookup of X, Y, and Z forces (F_X, F_Y, and F_Z, respectively) vs α, and L, M, and N vs β. The high α (greater than ± 20 deg) model uses various inputs of fuselage forces and moments at extreme angles (± 90 deg, ± 180 deg). These values are used in sine and cosine series expansions to give the forces and moments at any α or β. Reference 6 outlines this procedure clearly.

A rotor wake model has been written to determine the influence of the wake on the airframe. This model has been compared against test results presented in Ref. 8 and agrees fairly well with the reported values of rotor wake skew angle. This model may also be used for determining the rotor wake influence at the stub wing or the empennage.

Euler's Equations of Motion

Euler's equations of motion can be integrated to determine the response of the aircraft to the forces and moments acting on the helicopter previously discussed. Details of the dynamic analysis are discussed in Ref. 9 which presents an excellent derivation of Eqs. (3–8) describing aircraft motion

$$F_X = m(\dot{u}_f + Qw_f + Rv_f) \tag{3}$$

$$F_Y = m(\dot{v}_f + Pw_f + Ru_f) \tag{4}$$

$$F_Z = m(\dot{w}_f + Pv_f + Qu_f) \tag{5}$$

$$L = I_X\dot{P} + QR(I_Z - I_Y) - I_{XZ}(\dot{R} + PQ) \tag{6}$$

$$M = I_Y\dot{Q} + PR(I_X - I_Z) + I_{XZ}(P^2 - R^2) \tag{7}$$

$$N = I_Z\dot{R} + PQ(I_Y - I_X) - I_{XZ}(\dot{P} - QR) \tag{8}$$

where m is aircraft mass and I is the aircraft moment of inertia about the indicated body axis.

Equations (3–8) are nonlinear, and closed-form solutions exist for only the simplest of cases. The I_{XY} and I_{YZ} moments of inertia are considered negligible for most helicopters, and are not included. Without the use of digital computers, one usually linearizes these equations so their solutions can be examined. Such solutions are not useful in this investigation because the aircraft's response immediately following a tail rotor failure will usually violate the small angle and higher-order terms assumptions. Instead, the digital computer allows systematic numerical integration of the equations of motion while retaining nonlinearities. However, classical rotor theory was derived with two major assumptions regarding the wind axes and dynamic state of the rotor.

With the two assumptions above, it becomes apparent that the classical rotor theory, as described previously, will have to be modified to account for β, Q, and P. Classical rotor theory is derived assuming that the wind axis coordinate system (shown in Fig. 1) is identical to the body axis. Because of this, it is necessary to transform the cyclic controls, θ_1 and θ_2, to the wind axis when sideslip occurs. The wind axes and the transformed lateral and longitudinal cyclic control inputs are shown in Fig. 1 as θ_1' and θ_2', respectively. The changes in rotor flapping due to P and Q is accounted for using two closed-form equations for the changes in a_1 and b_1 which occur due to pitch and roll rates. These equations, which account for rotor inflow variation and coriolis forces, are derived in Ref. 10.

Simulation Validation

Dynamic response validation of the helicopter flight model is needed to assure correct response following a tail rotor failure. However, the purpose of this analysis is not to create a high-fidelity helicopter simulator or to solve the tail rotor failure problem, but to provide a tool which can be used to help analyze it. Thus, for this study, good correlation with flight tests and similar models is critical to ensure the accuracy of the helicopter flight model (i.e., to ensure that the tool, which is the product of this investigation, is useful). The model will also be compared to an existing AH-64A simulation program, FLYRT.[7,11] Comparison to FLYRT is important because it is considered to be the most accurate simulation model of the AH-64A available. The helicopter gross weight for each of the flight tests presented is about 14,600 lb. The c.g. position is approximately at the 203.5-in. station. The density altitude for each run is about 2000 ft. References 7 and 11 provide more detailed information about the exact conditions of each flight.

One of the more critical parts in validating the response to any control input is making sure that the helicopter is trimmed. However, the agreement of the trimmed angles is not as important as the balance of the forces and moments. The secant method (a numerical application of the Newton-Raphson iteration scheme) similar to the trimming method used in Ref. 6, is used. This method perturbs the system from the initial values for each control θ_0, θ_1, and θ_2 and tail rotor collective pitch, θ_{TR} which are initially input from a closed-form trim analysis. The resulting changes in the three moments and the residual Z force due to the perturbations are recorded in matrix form. Knowing the trimmed conditions (zero moments and balanced Z force), the inverse of this matrix is multiplied by the negative of the existing moments and excess vertical force, producing the required control inputs to trim the aircraft. Once the moments and residual Z force are eliminated, the aircraft assumes the pitch and roll angles which balance the X and Y forces, respectively. This slightly alters the balance achieved using the secant method, requiring iteration until trim is achieved.

The model in Ref. 6 occasionally experiences problems trimming the aircraft, however, no problems have been experienced trimming DYN at speeds less than or equal to approximately 130 kt. It should be noted that the number of iterations required to trim the aircraft using DYN increases significantly with forward speed.

The validation runs represent doublet inputs of θ_0, θ_1, and θ_2 at three different speeds: 1) hover, 2) flight in the "power bucket" at 80 kt, and 3) high-speed flight at 130 kt. These speeds were chosen to allow comparison between DYN and FLYRT. The FLYRT data presented are found in Ref. 7 with the exception of the hover collective doublet which is found in Ref. 11. A total of nine validation runs were made in this study, and the three runs presented are representative. It should be noted that actual swash plate inputs are used in the validation to avoid error in modeling the control system between the stick and swash plate. All main rotor controls angles presented from this point are swash plate inputs.

All control inputs are actual flight test time histories of the actuator deviation from the position at time zero. The three validation runs presented use a control doublet input which is an input disturbance from the trimmed control angle, followed by an opposite displacement approximately equal in magnitude and then returned back to the trimmed position.

Hover Collective Doublet

The agreement of normal acceleration response to a hover collective doublet (Fig. 2) appears to be very good, while the yaw axis response seems to be underpredicted. However, referring to the corresponding FLYRT curves, DYN and FLYRT match almost exactly. The flight test data may also contain some sources of error. Insight to this may be found in Ref. 7. The hover validation runs did not transform the controls to the wind axes due to the large fluctuations in β for very small changes in lateral velocity when V approaches zero.

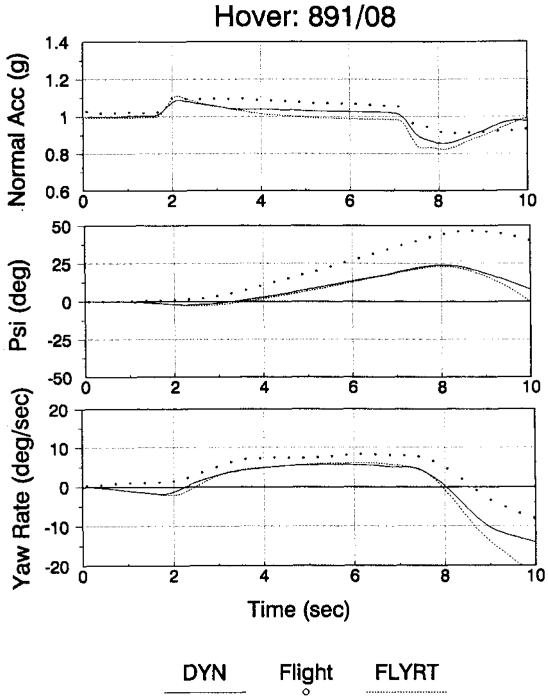

Fig. 2 Hover collective response validation.

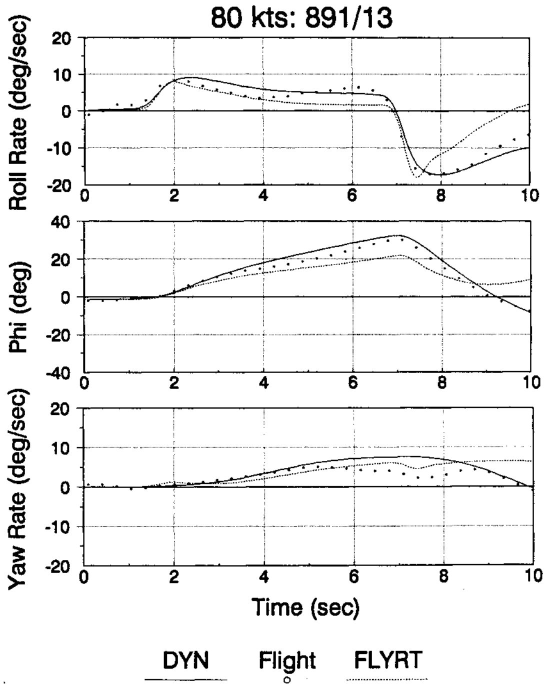

Fig. 3 80-kt Lateral cyclic response validation.

80-kt Lateral Cyclic Doublet

The 80-kt validation run, like the hover validation run in Fig. 2, represents response to a doublet control input. Figure 3 shows excellent agreement with flight test in roll rate response. DYN appears to predict the recovery more accurately than FLYRT. However, FLYRT predicts the dip in the yaw axis response, which DYN does not. This is probably because FLYRT contains a detailed engine model which allows the main rotor rotational speed to vary.

130-kt Longitudinal Doublet

Similar to the hover and 80-kt runs, the 130-kt validation plots show the response to a doublet control input. Figure 4 shows fair yaw axis response correlation with FLYRT, with

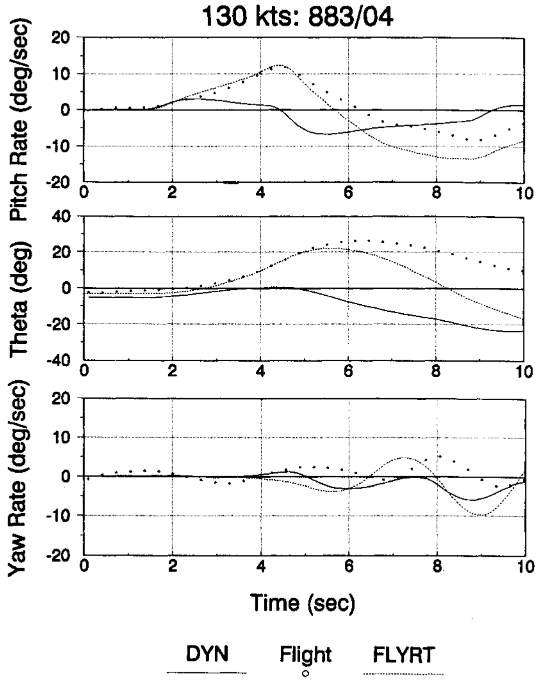

Fig. 4 130-kt Longitudinal cyclic response validation.

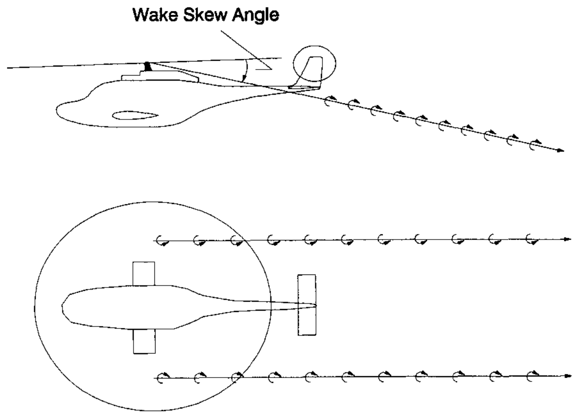

Fig. 5 Influence of rolled up main rotor wake.

the magnitude somewhat decreased. However, it shows a severe deficiency in predicting the pitch rate response. References 7 and 11 offer some insight to this problem. DYN does not assume any main rotor interference after the wake moves off of the stabilator around 70 kt. For this reason, a modification to the interference model in DYN was warranted.

As the helicopter gains forward speed, the wake of the helicopter begins to roll up into two distinct vortices, much like a fixed-wing aircraft. Thus, using basic vortex theory, the strength of the rolled-up vortices can be estimated using the relationship in Eq. (9).

$$\Gamma_0 = (T_{MR}/2\pi\rho V) \tag{9}$$

Figure 5 shows the orientation of the rolled-up main rotor wake with respect to the helicopter. Commensurate with an elliptic spanwise loading, the trailing vortices are assumed to be separated by a bound vortex of length $\pi D/4$ and originating from the same X-body station as the main rotor shaft. The vortices trail along the rotor wake skew angle which is calculated by the rotor wake model. The influence of this horseshoe vortex on the horizontal stabilator can then be calculated using the Biot-Savart law.[4] An empirical correction to this must be applied to the interference model to account for partial wake roll up until about 140 kt. So, for the AH-64A

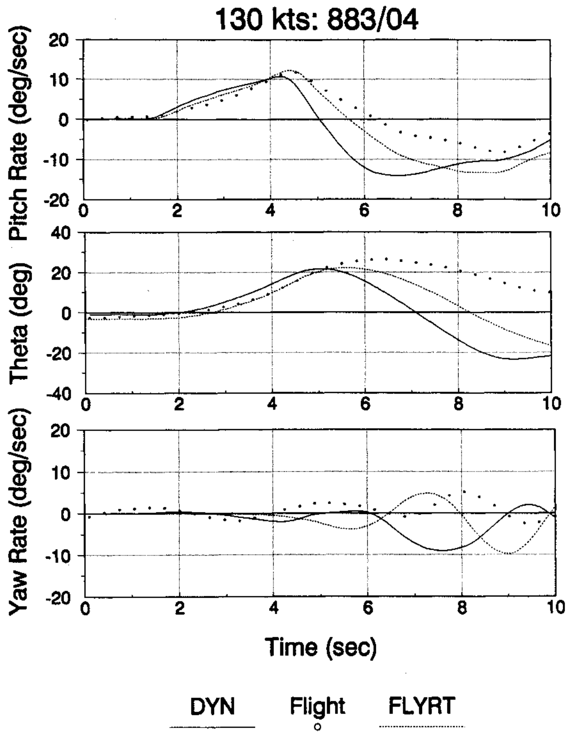

Fig. 6 Corrected 130-kt longitudinal cyclic response validation.

runs, the calculated induced velocity at the stabilator was increased linearly from 0% of calculated value at 70 kt to 100% of the calculated value using Eq. (9) at 140 kt.

Now, with the enhanced wake interference model in place, a new 130-kt longitudinal simulation can be run. Figure 6 shows much better pitch rate agreement between DYN and flight test than that observed in Fig. 4. The pitch rate response compares closely to the response predicted by FLYRT. Reference 11 details the wake interference model used in FLYRT, which includes an empirical flow survey around the empennage. The simple interference model described above, although less accurate than the model in FLYRT, is retained to preserve a generic helicopter simulation model. The collective and lateral cyclic response runs were repeated with the interference model in place and showed negligible differences.

Validation Summary

The helicopter simulation validation is fairly accurate at predicting helicopter response to all three of the main rotor pitch controls. This becomes especially apparent when the simplicity and speed of the model is considered, along with the generally good comparison to FLYRT, the industry standard AH-64A simulation model. There is some concern about the error in yaw rate phase from flight test which appears in both DYN and FLYRT. For this study, however, the frequency and magnitude of the response, which appear to match fairly accurately, are more critical when a tail rotor failure occurs.

Tail Rotor Failure Investigation

Tail rotor failure can happen in several ways. Two common types of failure are 1) loss of tail rotor pitch control and 2) complete loss of the tail rotor (tail rotor separation). The former was initially analyzed using validation runs where the controls were perturbed while the tail rotor controls remained at trim values. It became obvious that this type of failure would be a small deviation about the trim point where the controls failed, using collective pitch to yaw the aircraft. It is the latter type of failure, tail rotor separation, which represents the worst-case response and presents the most difficult control problems.

The following section presents the response of the helicopter following tail rotor separation from a trimmed aircraft at 80 and 130 kt. Following this section, logic is presented that represents the response of the closed loop recovery system which is the paper pilot in this investigation. Because the paper pilot represents ideal pilot response, the recovery system may more realistically be implemented using an automatic control system which could be engaged following a tail rotor failure. However, it is not the purpose of this study to develop a robust control system to be installed on the AH-64A which would allow it to recover from tail rotor failures. It is to develop a realistic model which can be used to explore recovery from a tail rotor failure in different helicopters during various flight conditions.

Controls-Frozen Failure

Initial analysis using DYN indicated that recovery from a tail rotor failure at speeds below approximately 80 kt (i.e., on the "back side" of the power curve) cannot be recovered while rotor power remains engaged. In fact, in most cases, the AH-64A operator's manual recommends autorotation for these flight conditions. For this reason, tail rotor failures below 80 kt will not be discussed. The controls were assumed frozen to show the potentially catastrophic nature of tail rotor failure if no control is taken, and to provide a basis for comparison.

Figure 7 shows the predicted response following a tail rotor separation at time zero from an AH-64A trimmed at 80 kt. The helicopter yaws nose right and loses altitude rapidly after 4 s. A large, fluctuating roll rate accompanies the yaw rate.

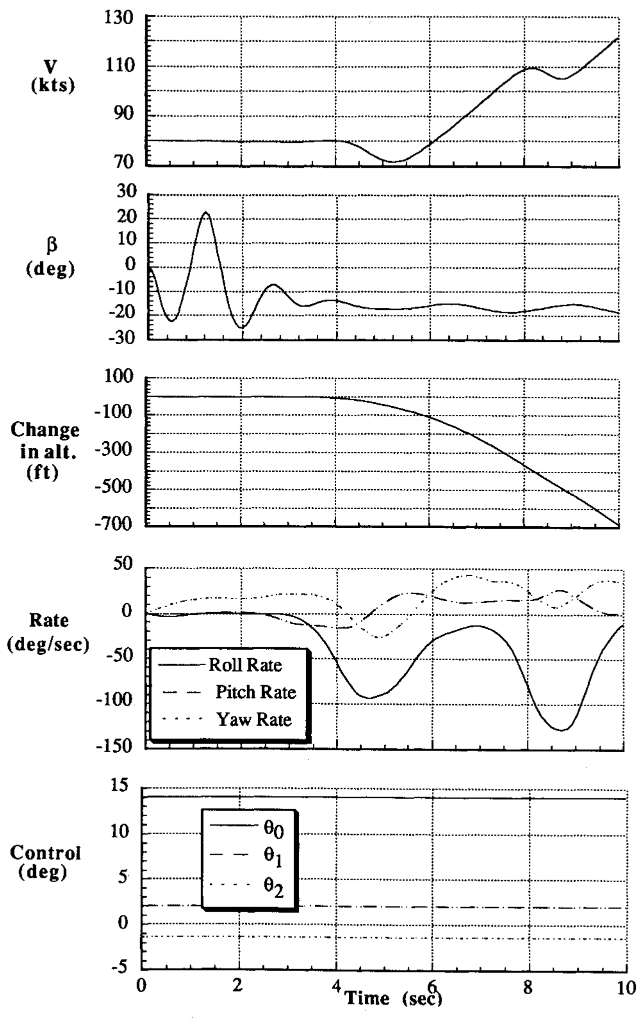

Fig. 7 Response after tail rotor separation at 80 kt, trimmed with controls frozen at trimmed settings.

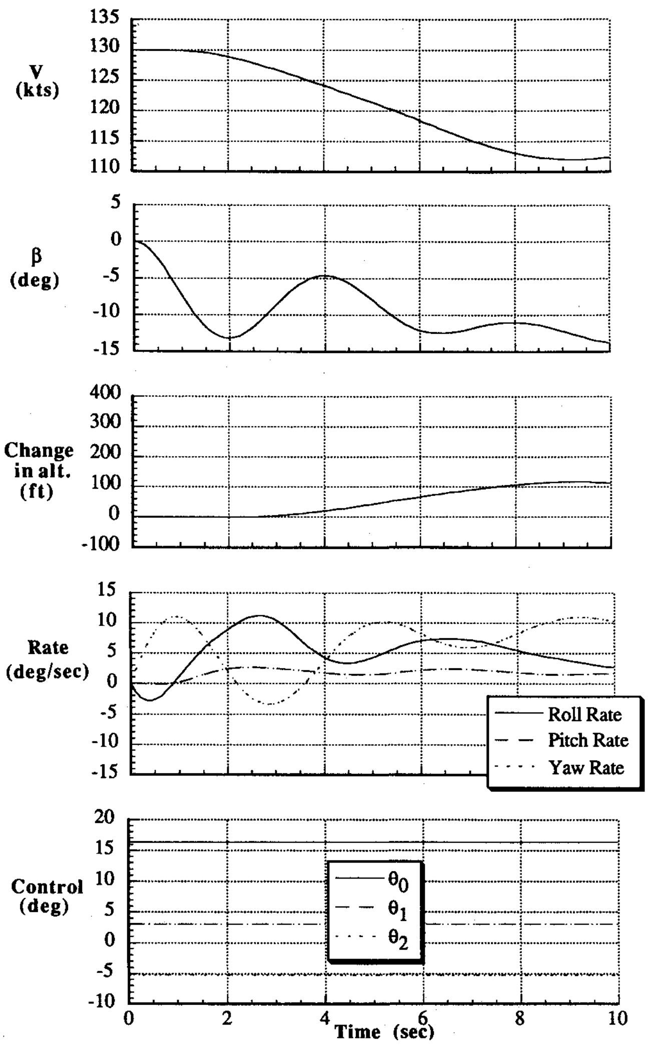

Fig. 8 Response after tail rotor separation at 130 kt, trimmed with controls frozen at trimmed settings.

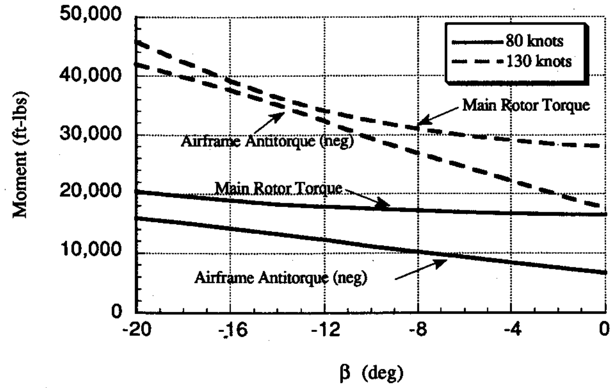

Fig. 9 Comparison of main rotor torque to airframe restoring moment with sideslip.

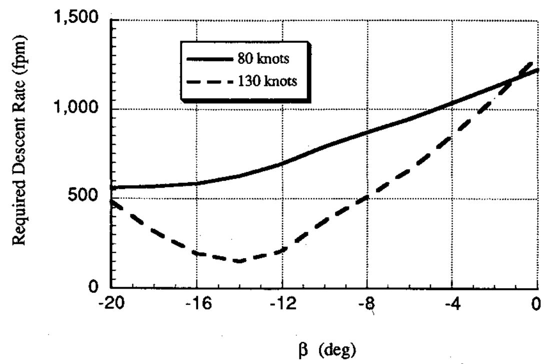

Fig. 10 Descent rate required to balance the excess main rotor torque with sideslip.

The roll rate is caused by the effective transformation of the cyclic controls as the magnitude of β increases, by the force generated by the vertical stabilizer, and by the inertial coupling of the roll and yaw axes.

Figure 8 shows the predicted response of the AH-64A trimmed at 130 kt following a tail rotor separation at time zero. The 130-kt response shows a drop in airspeed, coupled with a small gain in altitude. A fluctuation in roll rate again accompanies the yaw rate, however, both show much smaller magnitudes compared to the 80-kt case, due mostly to the increased effectiveness of the vertical stabilizer. Notice that the roll and yaw rates are now out of phase. A contributing factor may be the large increase in the aerodynamic moments compared to the moments generated by the roll-yaw inertial coupling relative to the 80-kt case. In general, the response during the first 10 s following a tail rotor separation at 130 kt is much less severe than the response at 80 kt in Fig. 7.

Tail Rotor Failure Recovery

The goal of the closed-loop recovery system is to obtain steady flight without a tail rotor. Examination of the available antitorque compared to the torque exerted on the airframe by the main rotor at different airspeeds is necessary. Figure 9 presents the torque and antitorque as a function of β at 80 and 130 kt. The analysis presented in Ref. 2 agrees well with these figures (although the AH-64A configuration used in this study has slightly less drag). Figure 9 shows antitorque deficiencies at all values of β up to negative 20 deg. Therefore, in a steady state, some descent rate is necessary to balance the torque and antitorque. Figure 10 shows the descent rate which achieves the torque balance for both 80 and 130 kt. The data in Fig. 10 were generated assuming that the torque reduction is equal to the descent rate (fps) multiplied by the helicopter gross weight (lb), and divided by the rotor rotational speed (rad/s). The descent rate data presented in Fig. 10 agree well with the conclusions made in Ref. 2. Figure 10 also indicates that a trimmed β of 20 deg at 80 kt and 15 deg at 130 kt would minimize the descent rate following a tail rotor separation in an AH-64A. With this information, the control system for recovery after a tail rotor separation will be formulated.

Response to the tail rotor failure is desired to be realistic, not only from a "hardware" point of view, but also to assure that real failure scenarios can be analyzed. For this reason, approximately 10 helicopter pilots were consulted at various stages during this study. They provided great insight on the various control aspects of helicopters, especially during emergency procedures.

It was determined that the control model should contain three basic items of logic: 1) a lag to account for pilot recognition of failure, and initial pedal response; 2) an initial "dump" of θ_0 and θ_2 to reduce main rotor torque and increase airspeed, respectively; and 3) control logic proportional to the state variables of the helicopter.

The control model is implemented in the existing flight model using three separate loops which correspond to the three parts above: 1) the LAG loop, 2) the DUMP loop, and 3) the CONTROL loop. Care was taken in these loops that the control actuator rate limits were not exceeded. Figure 11 presents a simplified flow chart showing the logic used to control the helicopter after a tail rotor separation.

The second part of the control loop, called the dump loop, is a desired instinctive pilot reaction in contrast to cutting engine power. Autorotation (cutting power) is not advisable following a tail rotor failure, unless the failure occurs close to the ground or at low speeds where powered recovery is

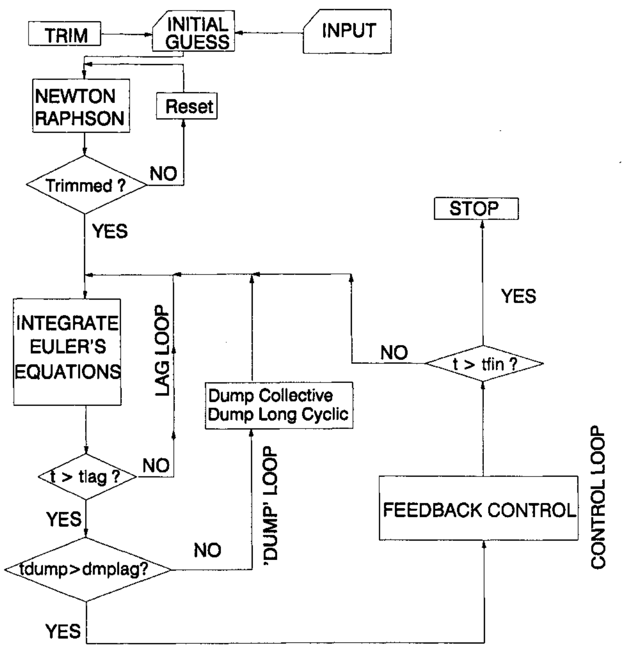

Fig. 11 Simplified flow chart showing control logic used in DYN.

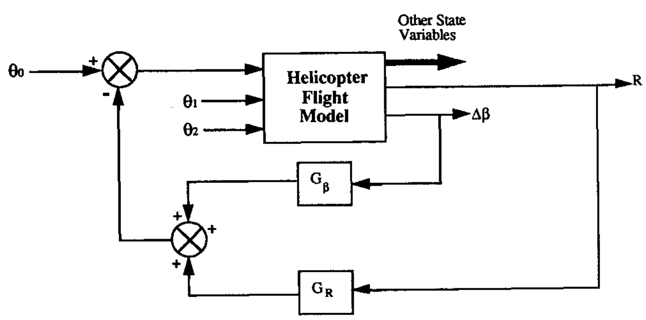

Fig. 12a Collective pitch feedback control system.

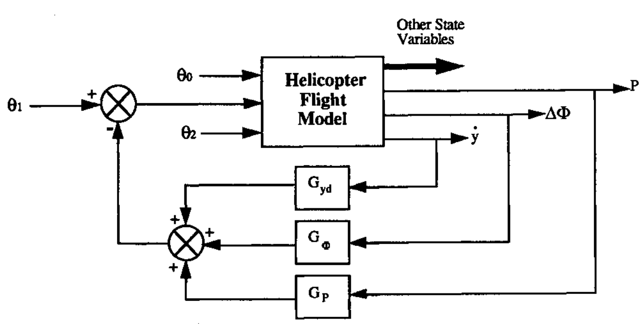

Fig. 12b Lateral cyclic pitch feedback control system.

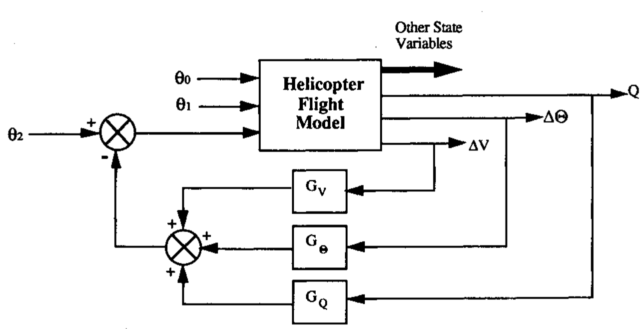

Fig. 12c Longitudinal cyclic pitch feedback control system.

not likely. The chance of getting the helicopter into an autorotative descent after simultaneously experiencing violent yawing, pitching, and rolling moments may not be possible without excessive loss of rotor speed. This is especially true for helicopters that have low inertia rotor systems such as the AH-64A.

Figures 12a–12c show block diagrams which describe feedback control on θ_0, θ_1, and θ_2, respectively. Although all controls are input to the helicopter flight model, they are separated in Fig. 12 for clarity. Figure 12a shows that gains on R and $\Delta\beta$ are fed back to θ_0 to trim β to the input value based on the steady-state predictions in Fig. 10. Figure 12b shows that gains on P, $\Delta\Phi$, and $\dot{y}$, are fed back to θ_1 to trim the roll angle and heading. Initially, the trim value of Φ is assumed zero until the roll oscillation decreases to a small amplitude (approximately 5 deg). When this occurs, the desired Φ is taken as the average value over the previous 10 s. Figure 12c shows that gains on Q, $\Delta\Theta$, and ΔV are fed back to θ_2 to trim Θ and maintain V. The trim value of Θ is determined using the same method as Φ outlined above. The values of the

Table 1 Feedback gain values

Gain	Value	Units
G_R	0.0001	s
G_β	0.0001	None
G_P	−20.0	s
G_Φ	−5.0	None
G_{yd}	−0.1	rad-s/ft
G_Q	20.0	s
G_Θ	5.0	None
G_V	0.2	rad-s/ft

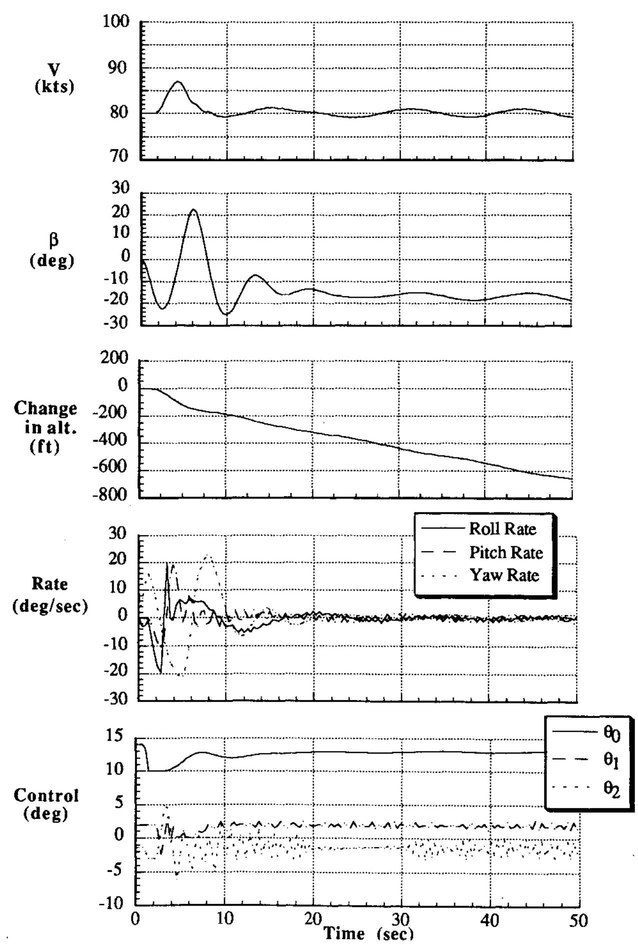

Fig. 13 Response following tail rotor separation at 80 kt, trimmed with failure recovery control system engaged.

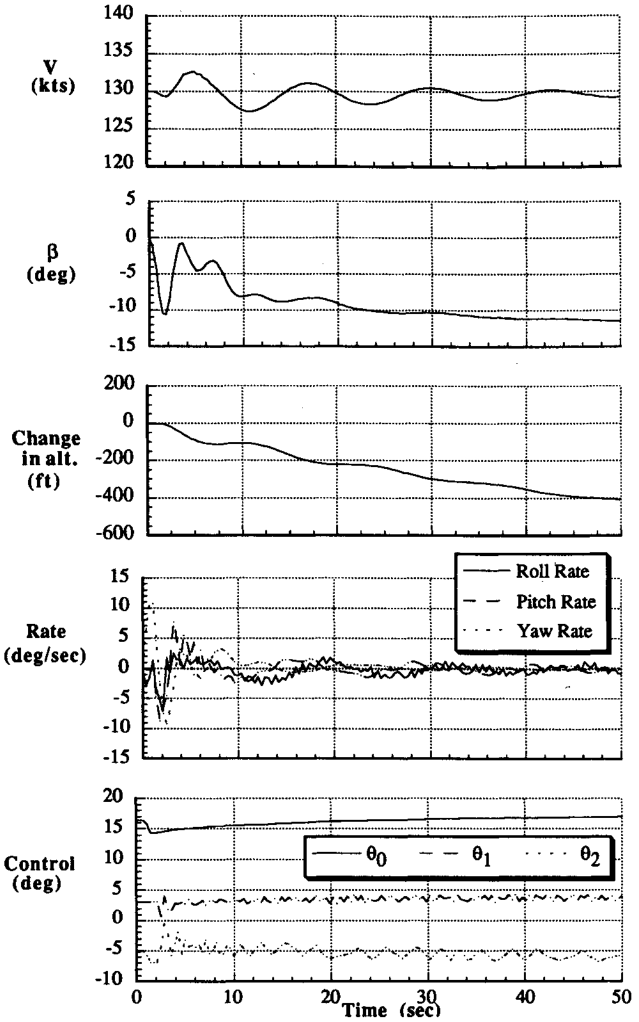

Fig. 14 Response following tail rotor separation at 130 kt, trimmed with failure recovery system engaged.

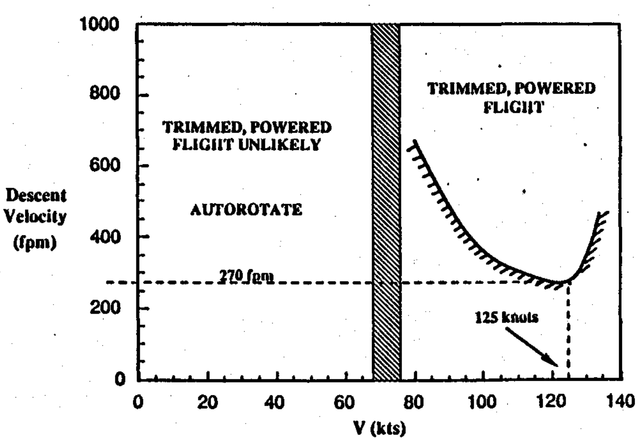

Fig. 15 Predicted minimum descent rate boundary required for steady flight in an AH-64A following tail rotor separation.

feedback gains were initially determined by estimating control sensitivities, and refined using trial and error. The gain values used are presented in Table 1. All of the recovery cases run used the same gain values.

Figure 13 shows the predicted response of an AH-64A trimmed at 80 kt to a tail rotor separation at time zero with the recovery system engaged. After 15–20 s, the helicopter reaches a steady descent of about 670 ft/min at a β of 17 deg. Notice that after 5 s the airspeed does not significantly deviate from the desired 80 kt. Figure 14 shows the predicted response of an AH-64A trimmed at 130 kt to tail rotor separation at time zero with the recovery system engaged. Like the 80-kt time history, after about 15–20 s, the helicopter is essentially in a steady-state descent of approximately 290 fpm at a β of 12 deg. Longer lag times would produce larger initial deviations of the state variables from the steady-state values, and if long enough, may cause divergence. It should be noted that the steady-state β was decreased in magnitude by approximately 3 deg from the values in Fig. 10 to eliminate short period (approximately 1 Hz) oscillations in β. If this closed-loop recovery system were to be used as an automatic control system, the initial lag time could be reduced to a small fraction of a second and the dump section removed.

Reference 2 estimates that the AH-64A would require between 500–1000 fpm descent to achieve trimmed flight with no tail rotor which is supported by the response in Fig. 13. Reference 2 also states that the AH-64A should be able to achieve steady, level flight at 125 kt without a tail rotor. Recovery runs at 125 kt, using DYN, predict that the AH-64A will have to descend at approximately 270 fpm to maintain trimmed flight without a tail rotor. This difference, although small, may be due to the fact that Ref. 2 presents a trim point which occurs at a single value of β. The ability of the control system to maintain steady flight at this point is unlikely, because of the instability with increasing negative β from the trimmed value. Thus, some descent rate is required to make the trim point a trim region where the torque and antitorque curves overlap. The difference may also be due, in part, to slight differences between the aerodynamic data used in this study and in Ref. 2.

Now that trimmed flight without a tail rotor has been demonstrated, it is valuable to present a flight envelope which can be used as a guideline to what descent rate should be sought at a given flight velocity if the tail rotor separates. Figure 15 shows the predicted descent rate envelope for the AH-64A in the event of tail rotor separation. Since DYN predicts that the AH-64A must maintain a descent at all airspeeds, after control recovery is achieved, an autorotation or run-on landing should be executed as soon as possible. Note that this envelope was generated using 1-s lag times.

Conclusions

The flight model, DYN, has shown that classical rotor theory can be used effectively in a 6 degree-of-freedom helicopter model, as long as the body aerodynamics are accurately described. This model predicts accurate first-order helicopter response to main rotor control inputs.

This investigation indicates that if the proper control response is not implemented, tail rotor separation from a trimmed helicopter at any speed is potentially catastrophic. This conclusion is drawn for all helicopters, even though the AH-64A was the only aircraft analyzed. This is because the AH-64A has a relatively large vertical stabilizer relative to most helicopters.

This study has shown that state variable feedback is an effective method to control the helicopter if tail rotor separation occurs between 80–130 kt. There is some minimum descent rate that the helicopter must maintain in order to trim the helicopter without a tail rotor in this speed range. This descent rate envelope will change for different aircraft configurations with different flat plate drag area and gross weight.

DYN is a tool which can be used to analyze tail rotor failure. The conclusions drawn about tail rotor failure using a model of the AH-64A agree with those made during initial testing of the AH-64A. DYN also shows great promise for use as a tool to model other kinds of failures and for basic helicopter simulation.

References

[1]Mainwaring, J. C., and Torres, C. B., "Projected Accident Costs for the LHX Aircraft," USASC TR 87-1, March 1987.

[2]Prouty, R. W., "Development of the Empennage Configuration of the YAH-64 Advanced Attack Helicopter," USAAVRADCOM TR-82-D-22, 1983.

[3]Gerdes, W. H., Jackson, M. E., and Beno, E. A., "Directional Control Development Experiences Associated with the UH-60A Utility Helicopter," USAAVRADCOM TR-82-D-26, 1983.

[4]McCormick, B. W., *Aerodynamics of V/STOL Flight*, Academic Press, New York, 1967.

[5]Gessow, A., and Crim, A., "A Theoretical Estimate of the Effects of Compressibility on the Performance of a Rotor in Various Flight Conditions," NACA TN 3798, 1956.

[6]Davis, J. M., Bennett, R. L., and Blankenship, B. L., "Rotorcraft Flight Simulation with Aeroelastic Rotor and Improved Aerodynamic Representation, Volume 1—Engineer's Manual," USAAMRDL TR 74-10A, June 1974.

[7]Kumar, S., Harding, J., and Bass, S., "AH-64 Apache Engineering Simulation Non-Real-Time Validation Manual," USAAVSCOM TR-90-A-010, Oct. 1990.

[8]Heyson, H., and Katzoff, S., "Induced Velocities Near a Lifting Rotor with Nonuniform Disk Loading," NACA TR 1319, 1957.

[9]Etkin, B., *Dynamics of Flight*, Wiley, New York, 1959.

[10]Prouty, R. W., *Helicopter Performance, Stability and Control*, PWS Engineering, Boston, MA, 1986.

[11]Harding, J. W., and Bass, S. M., "Validation of a Flight Simulation Model of the AH-64A Apache Attack Helicopter Against Flight Test Data," 46th Annual Forum of the American Helicopter Society, Washington, DC, May 1990.